

1 **Extending the CWM approach to intraspecific trait variation: how to deal**
2 **with overly optimistic standard tests?**

3

4 Running title: CWM-environment test extended for ITV

5

6 Authors: David Zelený^{1*}, Kenny Helsen² & Yi-Nuo Lee³

7 Institute of Ecology and Evolutionary Biology, National Taiwan University, Taiwan

8 *Corresponding author

9

10 36 pages; 9176 words, 1 table, 5 figures, 1 appendix

11 R-code and the real world dataset is on GitHub (<https://doi.org/10.5281/zenodo.5497773>)

12 **Keywords:**

13 trait-environment relationships

14 community level traits

15 Type I error rate

16 intraspecific trait variation

17 site-specific trait values

18 permutation test

19 response traits

20 environmental filtering

21

¹ zeleny@ntu.edu.tw

² helsenkenny@gmail.com

³ poiuytrewq976431@gmail.com

22 **Abstract**

23 Community weighted means (CWMs) are widely used to study the relationship between
24 community-level functional traits and environment variation. When relationships between
25 CWM traits and environmental variables are directly assessed using linear regression or
26 ANOVA and tested by standard parametric tests, results are prone to inflated Type I error
27 rates, thus producing overly optimistic results. Previous research has found that this problem
28 can be solved by permutation tests (i.e. the max test). A recent extension of this CWM
29 approach, that allows the inclusion of intraspecific trait variation (ITV) by partitioning
30 information in fixed, site-specific and intraspecific CWMs, has proven popular. However,
31 this raises the question whether the same kind of Type I error rate inflation also exists for
32 site-specific CWM or intraspecific CWM-environment relationships. Using simulated
33 community datasets and a real-world dataset from a subtropical montane cloud forest in
34 Taiwan, we show that site-specific CWM-environment relationships also suffer from Type I
35 error rate inflation, and that the severity of this inflation is negatively related to the relative
36 ITV magnitude. In contrast, for intraspecific CWM-environment relationships, standard
37 parametric tests have the correct Type I error rate, while being somewhat conservative, with
38 reduced statistical power. We introduce an ITV-extended version of the max test for the ITV-
39 extended CWM approach, which can solve the inflation problem for site-specific CWM-
40 environment relationships, and which, without considering ITV, becomes equivalent to the
41 “original” max test used for the CWM approach. On both simulated and real-world data, we
42 show that this new ITV-extended max test works well across the full possible magnitude of
43 ITV. We also provide guidelines and R codes of max test solutions for each CWM type and
44 situation. Finally, we suggest recommendations on how to handle the results of previously
45 published studies using the CWM approach without controlling for Type I error rate inflation.

46 **Introduction**

47 According to community assembly theory, which species will occur in a local community
48 partly depends on the result of environmental filtering by the prevailing local abiotic
49 conditions (Keddy 1992, Zobel et al. 1998). More recently, this environmental filtering is
50 believed to act directly upon species' functional response traits (Lavorel & Garnier 2002).
51 These traits consist of measurable properties of an individual organism that directly influence
52 its fitness under the prevailing environmental conditions (Violle et al. 2007). The realization
53 of this link between functional traits and the environment has opened up avenues to uncover
54 the mechanisms behind community assembly, and to predict community responses to
55 environmental change. This has resulted in an ever-increasing number of studies exploring
56 functional trait-environment relationships (e.g. Miller et al. 2019).

57 At the community level, trait-environment relationships are regularly assessed
58 through the calculation of community weighted mean trait values (CWMs) (Garnier et al.
59 2004, Diaz et al. 2007). The resulting CWMs are then usually directly related to different
60 environmental variables using correlation, regression, ANOVA or other general(ized) linear
61 mixed model techniques. We call this the *CWM approach* in this study. A number of
62 alternative methods are also available for assessing trait-environment relationships however,
63 including the fourth corner (Legendre et al. 1997, Dray & Legendre 2008, Peres-Neto et al.
64 2017), species' niche centroids (SNC; Peres-Neto et al. 2017, ter Braak et al. 2018) and
65 multilevel models (Brown et al. 2014, Jamil et al. 2013, Warton et al. 2015, Miller et al.
66 2019).

67 Traditionally, the CWM approach used fixed species-level trait values (a given
68 species has the same trait value in all occupied sites), and thus ignored intraspecific trait
69 variation (ITV), i.e. variation in trait values among individuals of the same species. This was
70 justified by the assumption that, in most datasets, the amount of ITV is negligible compared

71 to the amount of interspecific trait variation, i.e. variation among species (McGill et al. 2006).
72 However, this assumption has recently been challenged by several studies that found that
73 both within- and among-community ITV is often substantial, at least for plants (Albert et al.
74 2010, Messier et al. 2010, Siefert et al. 2015, Westerband et al. 2021). For other taxa, the
75 extent of ITV remains less well understood, however (e.g. Gaudard et al. 2019 for ants, Behm
76 and Kiers 2014 for arbuscular mycorrhizal fungi, or Dawson and Jönsson 2020 for
77 basidiomycetes). Consequently, researchers are now actively advocating the inclusion of ITV
78 in most community ecological trait research, including in trait-environment relationship tests
79 (Albert et al. 2011).

80 Specifically for CWM trait-environment relationships, studies have clearly illustrated
81 that results can be biased when using fixed species-level trait values instead of incorporating
82 ITV (Albert et al. 2012, Borgy et al. 2017). This has resulted in an increasing number of
83 studies where authors calculate CWMs using site- or habitat-specific trait values, measured
84 separately for each species in each site or habitat, respectively. Lepš et al. (2011) introduced
85 an extension of the CWM approach that allows the partitioning of the relative contribution of
86 ITV and interspecific trait variation to community-level trait-environment relationships. This
87 approach is based on the realization that CWMs calculated from fixed species-level trait
88 values (“fixed” CWM, excluding ITV) can vary among communities only if their species
89 composition differs (species turnover). On the contrary, differences in CWMs calculated
90 from site-specific trait values (“site-specific” CWM) can be caused by both species turnover
91 and ITV. The difference between the site-specific CWMs and fixed CWMs then only
92 encompasses the effect of ITV (“intraspecific variability effect” CWM, or “intraspecific”
93 CWM in short). These fixed, site-specific and intraspecific CWMs are subsequently related to
94 environmental variables using either regression or ANOVA and their explained variation is

95 partitioned between species turnover and ITV. This method has proven popular, and to date,
96 we have identified over 60 published case-studies using it.

97 Several studies recently found that the standard parametric tests in the CWM
98 approach using fixed trait values are prone to Type I error inflation, resulting in the situation
99 that even CWMs calculated from randomly generated species-level trait values often show
100 significant correlations to environmental variables (Peres-Neto et al. 2017, ter Braak et al.
101 2018, Zelený 2018). Peres-Neto et al. (2017) have shown that the correlation of CWMs and
102 environmental variables is in fact numerically tightly related to the fourth corner method
103 (introduced by Legendre et al. 1997), and that the same solution as used for controlling the
104 Type I error rate in the fourth corner (Dray et al. 2008, ter Braak et al. 2012), can be used to
105 control the inflated Type I error rate in the CWM approach. This solution is based on a
106 combination of two permutation tests, one permuting the sample attribute (i.e. the
107 environmental variable) and the other permuting the species attribute (i.e. the trait), into the
108 “max test”, by taking the higher (more conservative) P-value of the two permutations
109 (Cormont et al. 2011, ter Braak et al. 2012).

110 However, it is unclear if this Type I error inflation persists when introducing ITV in
111 the CWM approach following the method of Lepš et al. (2011). Up to date, none of the
112 papers using this method have tested, or tried to correct, for this potential Type I error
113 inflation. Note however, that Candeias and Fraterrigo (2020) and Sandel and Low (2019)
114 partly acknowledge, and try to address, related Type-I error inflation issues in their studies.
115 Part of the type I error problem for fixed CWMs arises because the CWMs of different sites
116 in a dataset are not independent, since sites usually share a least some species, and the trait
117 values of these shared species are identical. This lack of independence between fixed CWMs
118 reduces the effective degrees of freedom in the analysis of their relationship with
119 environmental variables. We expect that for site-specific CWMs this problem will be relaxed,

120 because the inclusion of ITV allows species to have different trait values in different sites,
121 thus reducing the dependence among sites. However, although ITV can be substantial, at least
122 for plants, it is often smaller than interspecific trait variation (cf. Messier et al. 2010, Siefert
123 et al. 2015, Westerland et al. 2021). We consequently expect that the use of site-specific trait
124 values will not completely remove the dependency issue, but that the severity of inflation will
125 depend on the magnitude of ITV. Moreover, the currently available max test solution cannot
126 be applied, because the vector-based trait permutation for fixed CWMs cannot readily be
127 extended to the site-by-species matrix for site-specific CWMs. For intraspecific CWMs, we
128 do not have enough clues to forecast whether they are or they are not affected by inflated
129 Type I error rate.

130 In this study, we explore 1) whether the CWM approach suffers from inflated Type I
131 error rates when including ITV, by calculating site-specific and intraspecific CWMs, 2)
132 whether this potential inflation depends on the magnitude of ITV, and 3) whether our newly
133 proposed modification of the max test can overcome this potential inflation problem. To
134 explore these questions, we quantified Type-I error rates for 1) simulated community data
135 with varying levels of intra- and interspecific trait variation, and 2) a real-world dataset
136 consisting of four functional leaf traits measured along a wind gradient for cloud forest
137 vegetation in northern Taiwan.

138 **Methods**

139 *Community weighted mean approach and extension for intraspecific trait variation*

140 When individual trait-environment relationships are analysed at the community level, three
141 objects are usually involved: a species composition matrix, an environmental variable (vector)
142 and a species trait (vector). Species composition is represented by a n -by- S matrix $\mathbf{L} = [l_{ij}]$,
143 where n is the number of sites (rows), S is the number of species (columns) and l_{ij} is the

144 contribution of species j to site i (where contribution can be expressed as abundance, biomass,
145 cover or another quantitative measure, or as presence-absence). The environmental variable is
146 represented by a n -elements-long vector $\mathbf{e} = [e_i]$, where e_i is the value of the environmental
147 variable for site i . The trait is represented by a S -elements-long vector $\mathbf{t} = [t_j]$, where t_j is the
148 trait value of species j . Naming conventions follow Peres-Neto et al. (2017), with a few
149 exceptions (explicitly mentioned further in the text) and several extensions.

150 The CWM approach first translates the species-level vector \mathbf{t} to a site-level vector $\mathbf{c} =$
151 $[c_j]$, by calculating the average trait value for a site across all present species, weighted by
152 each species contribution, as expressed in the matrix \mathbf{L} . The community weighted mean for
153 site i is calculated as

$$c_i = \sum_{j=1}^S p_{ij} t_j$$

154 where p_{ij} is the relative contribution of species j in site i , and t_j is fixed trait value of species j
155 (Garnier et al. 2004, Díaz et al. 2007). Relative contribution p_{ij} is calculated by dividing l_{ij} by
156 the sum of species contributions in site i for which trait values are available, i.e. as $p_{ij} =$
157 $l_{ij} / \sum_{j=1}^S l_{ij}$. Species with missing trait values should not be included in the calculation of
158 p_{ij} , so as the sum of relative species contributions in site i is always equal to one (Zelený
159 2018). Next, vector \mathbf{c} is directly related to the environmental vector \mathbf{e} by correlation,
160 regression, ANOVA or another method, and the significance of this relationship is often
161 tested.

162 Extension of CWM approach to allow the inclusion of ITV is done by distinguishing
163 site-specific and fixed trait values (Lepš et al. 2011). Site-specific trait values for species j in
164 site i thus become a n -by- S matrix $\mathbf{T} = [t_{ij}]$, where t_{ij} represents the mean trait value calculated
165 from individuals of species j collected within site i (the value is missing if the species does
166 not occur at the site or none of its individuals have been measured). The fixed trait values are

167 denoted as a n -elements-long vector $\bar{\mathbf{t}} = [\bar{t}_j]$, where \bar{t}_j is calculated as the mean of all site-
 168 specific trait values (t_{ij}) of species j across all n sites in the dataset where that species occurs.

169 Using the site-specific (\mathbf{T}) and fixed ($\bar{\mathbf{t}}$) trait values, Lepš et al. (2011) calculated site-
 170 specific CWMs, which include ITV as

$$c_i^{SS} = \sum_{j=1}^S p_{ij} t_{ij}$$

171 resulting in a n -elements-long vector $\mathbf{c}^{SS} = [c_i^{SS}]$, while fixed CWMs, which do not consider
 172 ITV, were calculated as

$$c_i^F = \sum_{j=1}^S p_{ij} \bar{t}_j$$

173 resulting in a n -elements-long vector $\mathbf{c}^F = [c_i^F]$, that is essentially c_i as calculated in the
 174 absence of ITV measurements (if we assume that $\bar{t}_j = t_j$). Finally, the intraspecific variability
 175 effect (called intraspecific CWM here) is defined as the difference between the site-specific
 176 CWM and the fixed CWM and calculated as $c_i^{ITV} = c_i^{SS} - c_i^F$, stored in a n -elements-long
 177 vector $\mathbf{c}^{ITV} = [c_i^{ITV}]$. Using the above formulas, calculation of \mathbf{c}^{ITV} can be rewritten to

$$178 \quad c_i^{ITV} = \sum_{j=1}^S p_{ij} (t_{ij} - \bar{t}_j) = \sum_{j=1}^S p_{ij} \Delta t_{ij}$$

179 where $\Delta t_{ij} = t_{ij} - \bar{t}_j$ are site-specific trait values centred by species, represented by a n -by- S
 180 intraspecific trait matrix $\Delta \mathbf{T} = [\Delta t_{ij}]$. Thus, unlike \mathbf{c}^{SS} , which quantifies the absolute CWM
 181 trait values observed at different sites, \mathbf{c}^{ITV} only quantifies the contribution of ITV to site-
 182 specific CWMs.

183 Lepš et al. (2011) pointed out that changes in site-specific CWMs (\mathbf{c}^{SS}) are caused
 184 either by species composition turnover (quantified by \mathbf{c}^F), changes in species-level trait values,
 185 i.e. ITV (quantified by \mathbf{c}^{ITV}), or by both. They proposed a method to partition the effect of
 186 these two sources, in which \mathbf{c}^{SS} , \mathbf{c}^F and \mathbf{c}^{ITV} are separately related to the vector \mathbf{e} using a

187 general linear model approach. The sum of squares (SS) are then extracted from each model,
188 where SS_{specific} represents the total among-site trait variation explained by the environmental
189 variable ($\mathbf{c}^{\text{SS}} \sim \mathbf{e}$), while SS_{fixed} and SS_{intra} represent the contribution of species turnover ($\mathbf{c}^{\text{F}} \sim$
190 \mathbf{e}) and ITV ($\mathbf{c}^{\text{ITV}} \sim \mathbf{e}$), respectively. If the effects of species turnover and ITV vary
191 independently, $SS_{\text{specific}} = SS_{\text{fixed}} + SS_{\text{intra}}$. Usually, however, the effects of species turnover
192 and ITV covary, either positively (i.e. when \mathbf{c}^{F} and \mathbf{c}^{ITV} both have either a positive or a
193 negative response to the environmental variable) or negatively (i.e. when \mathbf{c}^{F} and \mathbf{c}^{ITV} respond
194 oppositely to the environmental variable). Lepš et al. (2011) therefore suggested to add a
195 covariation component, calculated as $SS_{\text{cov}} = SS_{\text{specific}} - SS_{\text{fixed}} - SS_{\text{intra}}$. This approach has
196 been implemented in the R package *cati* (Taudiere & Violle 2015).

197 *Type I error inflation for trait-environment relationships in the CWM approach*

198 Previous studies have shown that using the CWM approach without considering ITV (thus
199 using the fixed CWM vector \mathbf{c}^{F}) to assess the link between environment and traits often
200 results in Type I error inflation. This is explained by the fact that a true link between traits
201 and environment ($\mathbf{t} \leftrightarrow \mathbf{e}$) can only occur if both the link between environment and species
202 composition, and the link between traits and species composition are present ($\mathbf{e} \leftrightarrow \mathbf{L}$ and $\mathbf{t} \leftrightarrow \mathbf{L}$,
203 respectively). Type I error inflation then occurs when the environment, but not traits, are
204 related to the species composition (i.e. $\mathbf{e} \leftrightarrow \mathbf{L}$ and $\mathbf{t} \nleftrightarrow \mathbf{L}$, Peres-Neto et al. 2017). The solution
205 to this inflation problem was adopted for the CWM approach by Peres-Neto et al. (2017)
206 from an analogous solution applied in the fourth-corner approach (Legendre et al. 1997; Dray
207 & Legendre 2008). It consists of calculating two permutation tests, one permuting the rows in
208 \mathbf{L} to test the $\mathbf{e} \leftrightarrow \mathbf{L}$ link, and one permuting the columns in \mathbf{L} , to test the $\mathbf{t} \leftrightarrow \mathbf{L}$ link. Both tests
209 are then combined together into the “max test” by only taking the largest P-value (least
210 significant result) as the test of the $\mathbf{t} \leftrightarrow \mathbf{e}$ link (Cormont et al. 2011, ter Braak et al. 2012). An

211 equivalent result is achieved by replacing the row-based permutation of the \mathbf{L} matrix by
212 permuting vector \mathbf{e} and relating it to vector \mathbf{c}^F (calculated from not-permuted trait values \mathbf{t}),
213 and replacing the column-based permutation test of \mathbf{L} by permuted trait values \mathbf{t} , and relating
214 the newly resulting vector ${}^P\mathbf{c}^F$ (where P stands for permuted) to the not-permuted vector \mathbf{e} (Fig.
215 1; Zelený 2018). For convenience, we still refer to these permutation schemes as row- and
216 column-based permutations, respectively.

217 *Simulated community data with ITV*

218 To assess whether the CWM approach extended for ITV inclusion has a correct Type I error
219 rate, we simulated community data that included intra- and interspecific trait variation that
220 was directly structured by a hypothetical environmental gradient. More specifically, we
221 evaluated the potential type I error inflation for the linear regressions between vectors \mathbf{c}^F , \mathbf{c}^{SS}
222 or \mathbf{c}^{ITV} , on the one hand and vector \mathbf{e} , on the other hand.

223 To generate simulated compositional data structured by an environmental variable (\mathbf{e})
224 we used the COMPAS model proposed by Minchin (1987) and extended by Fridley et al.
225 (2007). The extended model allows the creation of a simulated community by generating S
226 unimodal species response curves along a vector \mathbf{e} of fixed length, where each species
227 response curve (represented by a Beta function, Minchin 1987) quantifies the probability with
228 which a random individual found at a given gradient location is assigned to that given species.
229 The species composition of individual sites is then generated by randomly selecting n
230 locations along the environmental gradient, and assigning a predefined number of individuals
231 to different species at each site, according to the species (response-curve-defined) occurrence
232 probability at that site. In our simulation, we set the number of species $S = 50$, number of
233 sites $n = 25$, and 100 individuals sampled in each site. The width of each species response
234 curve (one of the parameters of the Beta function) is generated as a random number from a

235 uniform distribution between 0 and the total length of the environmental gradient. This length
236 was set at 5000 units, but sites were only allowed to be sampled between 500 and 4500 units
237 to avoid gradient edges with a lower density of species response curves. The simulation
238 model returns two objects: a vector \mathbf{e} (positions of sites along the gradient), and a n -by- S
239 composition matrix \mathbf{L} (with numbers in cells representing the counts of individuals of a given
240 species in a given site). This simulation was performed 50 times with the same number of
241 species and sites, resulting in 50 independent sets of \mathbf{e} and \mathbf{L} .

242 For each simulation, we generated a matrix of simulated site-specific trait values \mathbf{T} , in
243 which both interspecific and intraspecific trait variation was completely, positively linked to
244 vector \mathbf{e} . The n -by- S matrix \mathbf{T} was generated by replacing each non-zero value of l_{ij} in a site i
245 of matrix \mathbf{L} by the value e_i (zero values of l_{ij} became missing values in \mathbf{T}). In $\mathbf{T} = [t_{ij}]$,
246 different species occurring in the same site will have the same t_{ij} value, and the same species
247 occurring in different sites can have different t_{ij} values. Finally, we rescaled all values in \mathbf{T}
248 into the range between 0 and 1, and added a small value (generated as a random number from
249 a uniform distribution between -0.1 and 0.1) as a random noise to each t_{ij} .

250 We included an extra step that allowed modifying the magnitude of ITV in the
251 simulated matrix \mathbf{T} . For this, we first calculated the vector of fixed trait values $\bar{\mathbf{t}}$ as the means
252 of individual columns of matrix \mathbf{T} , and calculated the matrix $\Delta\mathbf{T} = [\Delta t_{ij}] = [t_{ij} - \bar{t}_j]$. Then
253 we introduced coefficient m to control the magnitude of simulated ITV in a matrix of site-
254 specific trait values $\mathbf{T}^m = [t_{ij}^m] = [m\Delta t_{ij} + \bar{t}_j]$. For each simulated vector \mathbf{e} and matrix \mathbf{L} we
255 generated a set of site-specific trait matrices \mathbf{T}^m for m ranging from 0 to 5 with 0.5 intervals.
256 If $m = 0$ (no ITV) all values of t_{ij} in column j are identical, and equal to \bar{t}_j ; this matrix was
257 reduced into the vector $\bar{\mathbf{t}}$ and used as fixed trait values. Increasing m increases the magnitude
258 of ITV (for $m = 1$, the values in t_{ij} are identical to those calculated from \mathbf{L} and \mathbf{e} , as
259 described earlier). Additionally, we also constructed a simulated \mathbf{T}^m matrix in which the trait

260 values were random values drawn from a standard normal distribution, $N(0, 1)$; no random
261 noise was added to t_{ij} value in this scenario. The latter scenario (with notation $m = \infty$ used in
262 the following text) represents a situation in which the site-specific trait value of a given
263 species is a random sample from the full pool of potential trait values across all species,
264 unconstrained by any species-specific ITV range. Thus, in total we have one vector of fixed
265 trait values $\bar{\mathbf{t}}$ and 11 site-specific trait matrices \mathbf{T}^m for each simulation.

266 *Dependence of the Type I error rate on the magnitude of ITV*

267 To assess the Type I error rates of the linear regressions of \mathbf{c}^F , \mathbf{c}^{SS} or \mathbf{c}^{ITV} to vector \mathbf{e} , tested by
268 parametric F -tests using our simulated community data, we first cancelled the link between
269 the traits and the species composition by permuting the trait matrices for each separate
270 simulation (Fig. S1). For the fixed trait values, we permuted values within vector $\bar{\mathbf{t}}$ to get ${}^P\bar{\mathbf{t}} =$
271 $[{}^P\bar{t}_j]$ (Fig. S1). For the intraspecific trait values, we calculated the intraspecific trait matrix
272 $\Delta\mathbf{T}^m$ for each \mathbf{T}^m and permuted the values within each column (species) of $\Delta\mathbf{T}^m$ to get ${}^P\Delta\mathbf{T}^m$
273 $= [{}^P\Delta t_{ij}]$. Note that these column permutations are only performed across cells where the
274 species is present. Finally, vector ${}^P\bar{\mathbf{t}}$ and matrix ${}^P\Delta\mathbf{T}^m$ were combined into a matrix of
275 permuted site-specific trait values ${}^P\mathbf{T}^m = [{}^P t_{ij}] = {}^P\Delta t_{ij} + {}^P\bar{t}_j$. Subsequently, ${}^P\bar{\mathbf{t}}$, and all ${}^P\mathbf{T}^m$ and
276 ${}^P\Delta\mathbf{T}^m$ matrices were combined with the \mathbf{L} matrix to calculate one ${}^P\mathbf{c}^{SS}$, 11 ${}^P\mathbf{c}^F$ and 11 ${}^P\mathbf{c}^{ITV}$
277 vectors, respectively. Each of these 23 CWM vectors was then regressed against vector \mathbf{e} and
278 significance levels assessed by parametric F -tests. We repeated all trait matrix permutations
279 1000 times, and for each of the 23 trait- environment regressions we counted the number of
280 significant correlations ($p < 0.05$) (N_{obs}). Since the null hypothesis that the trait is not
281 correlated to the environmental variable is true, because we broke the link between the trait
282 and the species composition by permuting trait values, the expected number of significant
283 correlations (i.e. the Type I error rate) is $\alpha(0.05) \times 1000 = 50$ (N_{exp}). The Type I error rate

284 inflation was then quantified using the inflation index $I(\alpha) = N_{\text{obs}}/N_{\text{exp}}$ (Lennon 2000); an
285 index value of 1 indicates no inflation.

286 Finally, the mean \pm SD inflation index across the 50 simulations was plotted against
287 the magnitude of ITV in the simulated data (cf. parameter m), separately for P_{C}^{SS} , and $P_{\text{C}}^{\text{ITV}}$.
288 To allow comparison with real datasets, we transformed parameter m to “relative ITV index”,
289 calculated as the mean variance of ITV (i.e. variance of individual species’ site-specific trait
290 values across all sites, averaged across species) divided by the variance of interspecific trait
291 variation across all species included in the analysis (calculated from the fixed trait values).
292 This ratio is equivalent to the $T_{\text{PC/PR}}$ T-statistic introduced by Violle et al. (2012).

293 *Introducing a max solution for the ITV-extended CWM approach*

294 The previously described row- and column-based permutation tests used for controlling Type
295 I error inflation in the CWM approach (Peres-Neto et al. 2017, ter Braak et al. 2018) cannot
296 be directly used for the ITV-extended CWM approach (Lepš et al. 2011). While the row-
297 based permutation test can still be performed by permuting vector \mathbf{e} (Fig. 2a), it is not clear
298 how the column-based permutation test should permute trait values in the trait matrix \mathbf{T} ,
299 opposed to vector $\bar{\mathbf{t}}$ used in the absence of ITV. Both the species composition matrix (\mathbf{L}) and
300 the site-specific trait matrix (\mathbf{T}) usually contain some sites i where species j is absent ($p_{ij} = 0$)
301 and thus the site-specific trait value is not available ($t_{ij} = \text{NA}$). Permuting columns in \mathbf{T}
302 (analogously to permuting elements in \mathbf{t}) would mismatch values in these two matrices,
303 causing some species with non-zero abundances in \mathbf{L} being newly paired with missing site-
304 specific trait values in \mathbf{T} and vice versa. To avoid this problem, we propose a new max test
305 version containing a column-based permutation test that combines separate interspecific (on
306 vector $\bar{\mathbf{t}}$) and intraspecific (on matrix $\Delta\mathbf{T}$) trait permutations. For vector $\bar{\mathbf{t}}$ the fixed trait
307 values are directly permuted to obtain $P\bar{\mathbf{t}}$. The permutation of values in $\Delta\mathbf{T}$, however, is done

308 separately for each column (ignoring cells with missing values) to get ${}^P\Delta\mathbf{T}$. The permuted
309 mean trait values in vector ${}^P\bar{\mathbf{t}}$ and permuted site-specific trait matrix ${}^P\Delta\mathbf{T}$ are then combined
310 together into a new matrix of permuted site-specific trait values ${}^P\mathbf{T}$. This new matrix is then
311 used to calculate ${}^P\mathbf{c}^{SS}$, which is then related to the non-permuted vector \mathbf{e} (Fig. 2b). The final
312 max test then combines the row-based permutation test (using ${}^P\mathbf{e}$) and the new column-based
313 permutation test (using ${}^P\mathbf{c}^{SS}$) by only taking the largest P-value (least significant result),
314 similarly as the previously described max test for the CWM approach without extension for
315 ITV (Cormont et al. 2011, ter Braak et al. 2012).

316 We explored whether this newly proposed max test for ITV-extended CWM approach
317 can correctly control for Type I error rate inflation for our 50 simulations, across different
318 magnitudes of ITV. For this, we used the same 50 simulated datasets we used to quantify
319 inflation of Type I error rate. For fixed CWM ($m = 0$), we replaced this newly modified
320 column-based test by a test permuting only the mean trait values in $\bar{\mathbf{t}}$ (Fig. 1b). We repeated
321 1000 times each test for each combination of dataset and ITV magnitude, and plotted the
322 average and standard deviation of the inflation index across the 50 simulations for each test
323 against the ratio of intra- and interspecific trait variation, as described earlier.

324 *Real world dataset: leaf traits of woody species in the cloud forest of Taiwan*

325 To illustrate the effect of ITV on community-level trait-environment relationships in a real-
326 world dataset, we used data from the one-hectare vegetation plot in the cloud zone of
327 northern Taiwan (24°42'25" N, 121° 26'29" E, 1758-1782 m a.s.l.), hereafter termed the
328 Lalashan Forest Dynamics Plot. The plot is located on a wide mountain ridge, with several
329 dry gullies and a windward slope in the eastern part of the plot. The vegetation is defined as
330 *Chamaecyparis montane* mixed cloud forest (Li et al. 2013), with coniferous cypress
331 *Chamaecyparis obtusa* var. *formosana* dominating the canopy, and several evergreen broad-

332 leaf tree species dominating the subcanopy (e.g., *Neolitsea accuminatissima*, *Quercus*
333 *sessilifolia*, *Rhododendron formosanum*, *Trochodendron aralioides*). Within the 100 m × 100
334 m Lalashan Forest Dynamics Plot, established following ForestGeo protocol (Condit 1988),
335 we surveyed woody species in 25 systematically distributed 10 m × 10 m subplots. We
336 recorded diameter at breast height (DBH) and species identity of all woody individuals with a
337 DBH ≥ 1 cm, and used relative number of individuals and relative basal area (derived from
338 DBH) to calculate the importance value index (IVI) per subplot for each species (Curtis
339 1959). IVI values were then organized in the subplot × species **L** matrix. In total, we
340 surveyed 1110 individuals of 49 species (including 48 broad-leaved and one coniferous
341 species).

342 For 1–3 individuals of each broad-leaved species within each subplot, we collected
343 three mature leaves for trait measurements. For each leaf, we measured leaf area (LA, mm²),
344 specific leaf area (SLA, mm²/mg), leaf dry matter content (LDMC, mg/g) and leaf thickness
345 (Lth, mm), following the protocols of Pérez-Harguindeguy et al. (2013). Leaf-level trait
346 values were first averaged per individual and subsequently per species in each subplot, to
347 obtain a species × site-specific trait values **T** matrix. Since the distribution of site-specific
348 trait values of LA and SLA was strongly right-skewed, we log₁₀-transformed them before
349 further analysis. We measured leaf traits for 665 individuals of all 48 broad-leaf species.

350 For each subplot, we also calculated a set of topographical parameters, including
351 mean elevation (m), convexity (m) and windwardness. Mean elevation of the subplot and
352 convexity were calculated from the elevation of corner piles, following Valencia et al. (2004).
353 Windwardness is a combination of aspect and slope, expressed as ‘easterness’ × slope, where
354 ‘easterness’ is the aspect folded along the east-west axis, rescaled into +90° for the E and -
355 90° for the W direction. Windwardness is expected to be related to the effect of the chronic
356 north-eastern (winter) monsoon winds. We additionally calculated a hypothetical

357 ‘environmental’ factor that was directly calculated from the \mathbf{L} matrix. This variable, the
358 subplot scores on the first ordination axis of a correspondence analysis calculated on the \mathbf{L}
359 matrix (hereafter named CA1), presents the strongest possible predictor of subplot-level
360 species composition, since it is directly derived from it.

361 We used data from this case study for two subsequent analyses. In the first one, we
362 evaluated the relationship between Type I error inflation and the magnitude of ITV, for the
363 four measured leaf traits and the two environmental factors, windwardness and CA1. We
364 calculated Type I error rates for the relationships (linear regression, F -test) between the four
365 site-specific and intraspecific CWMs, on the one hand, and windwardness and CA1, on the
366 other hand (we did not consider the fixed CWMs in this analysis). Species for which no trait
367 measurements were performed were removed from \mathbf{L} matrix. The two CWM vectors, \mathbf{c}^{SS} and
368 \mathbf{c}^{ITV} , were calculated as defined earlier. To break the relationship between traits and
369 environment in this data, we permuted site-specific and intraspecific trait data and performed
370 10,000 independent permutations to quantify the inflation index, as described earlier. For
371 each trait, we also calculated the relative ITV index and plotted the inflation index for each
372 tested community-level trait–environment relationship against the relative ITV index. For
373 site-specific CWMs, we additionally assessed if applying our newly introduced ITV-extended
374 max test (with 999 permutations) could remove Type I error inflation.

375 In the second analysis, we used the variation partitioning method introduced by Lepš
376 et al. (2011) and modified by Fajardo & Siefert (2018) for linear regression, to explore the
377 specific community-level trait–environment relationships in our dataset and to quantify the
378 effects of ITV, species turnover and their interaction on these relationships. We used all four
379 measured leaf traits and the three measured topographical variables (but not CA1). For each
380 trait and topographical variable combination, we calculated three linear regression models
381 and tested them using the appropriate method: (i) $\mathbf{c}^{\text{F}} \sim \mathbf{e}$, tested by the “original” max test, (ii)

382 $\mathbf{c}^{SS} \sim \mathbf{e}$, tested by the newly introduced ITV-extended max test, and (iii) $\mathbf{c}^{ITV} \sim \mathbf{e}$, tested by the
383 standard parametric F -test. For (i) and (ii), we also included standard parametric F -tests to
384 allow comparison of the results with the correct test method (max test). We decided not to
385 correct for multiple testing issue in this analysis, as we mainly compare differences between
386 P -values calculated by standard parametric test and max permutation tests for individual trait-
387 environment combinations. For each regression, we then calculated the sum of squares,
388 where SS_{fixed} represents the effect of species turnover, SS_{specific} the total trait variation, and
389 SS_{ITV} the effect of ITV, respectively. We subsequently partitioned those variations by the
390 formula $SS_{\text{specific}} = SS_{\text{fixed}} + SS_{\text{ITV}} + \text{covariation}$. All sum of square values were then rescaled
391 to percentage scale, where SS_{specific} was set to 100%.

392 All calculations with the simulated and real world datasets were performed in R 4.0.4.
393 (R Core Team 2021). The R code and the real world data set are provided at
394 <https://doi.org/10.5281/zenodo.5497773>. The simulated datasets were generated using the
395 *simcom* package (Zelený, version 0.1.0, <https://github.com/zdealveindy/simcom>), max
396 permutation tests for the fixed CWM-environment relationships were performed with the
397 *weimea* package (Zelený, version 0.1.18, <https://github.com/zdealveindy/weimea>),
398 correspondence analysis with the *vegan* package (Oksanen et al., version 2.5-7) and the
399 partitioning of among-plot trait variation with functions modified from the *cati* package
400 (Taudiere & Violle, 2015, version 0.99.3).

401 **Results**

402 *Simulated community data*

403 The relationships between site-specific CWMs and environment, tested using standard
404 parametric tests, have an inflated Type I error rate, where the inflation is negatively related to
405 the magnitude of ITV (Fig. 3a). Type I error inflation is highest at the smallest relative ITV

406 index, approaching the inflation for fixed CWM. The inflation seems to be almost absent if
407 the relative ITV index is higher than 3, and there is no obvious inflation ITV is unconstrained
408 ($m = \infty$). The relationship between intraspecific CWMs and environment, tested using
409 standard parametric tests, does not have an inflated Type I error rate (Fig. 3b), and
410 consequently shows no relationship with the relative ITV index. This test actually seems
411 rather conservative, with all inflation index values below one.

412 Our newly introduced ITV-extended max test successfully controls for Type I error
413 rate inflation of site-specific CWMs for all magnitudes of ITV (Fig. 3c). For fixed CWMs
414 (ITV = 0), this test reverts to the “original” max test, which also controls for Type I error rate
415 inflation (Fig. 3c). The relationship of intraspecific CWMs and environment was not inflated
416 when tested by standard parametric *F*-tests, so no permutation-based correction was
417 necessary.

418 *Leaf traits of woody species in the cloud forest*

419 Regression of site-specific CWMs against the two environmental variables (the measured
420 windwardness and generated CA1) showed an inflated Type I error rate for all four measured
421 traits (Fig. 4a). The inflation index values were, overall, higher for regressions against CA1
422 compared to windwardness. While the inflation index showed a somewhat decreasing trend
423 with increasing relative ITV for CA1, no relationship was observed for windwardness. All
424 regressions of intraspecific CWMs against CA1 and windwardness had an inflation index
425 close to 1, with no apparent trend along the increasing relative ITV index (Fig. 4b). The
426 newly introduced ITV-extended max test also successfully addressed the type I error inflation
427 in this dataset (inflation index close to or lower than 1).

428 From the CWM-environment relationships in our dataset which were significant ($P <$
429 0.05) when tested by *F*-test, several became insignificant following max test correction (Tab.

430 1). For site-specific CWMs, Lth was positively and SLA negatively related to windwardness
431 (Fig. 5b and c, respectively) based on both the parametric and max tests (Table 1). For fixed
432 CWMs, LA was positively related to elevation and SLA negatively related to convexity when
433 tested with parametric tests, but based on the max test, both relationships are only marginally
434 significant ($P < 0.1$) (Table 1). Finally, for the intraspecific CWMs (tested only by parametric
435 test), we found a negative relationship with windwardness for both LA and SLA (Fig. 5a&c)
436 and a positive relationship between Lth and windwardness (Fig. 5b). None of the three
437 CWMs for LDMC were significantly related to any measured environmental variable.
438 Variance partitioning of the trait – environment relationship into the effect of species
439 turnover, ITV and their covariation showed that there is a considerable positive covariation
440 fraction for the SLA and Lth relationships with windwardness (Fig. S2).

441 **Discussion**

442 We illustrate with both simulated and real community data that testing community-level trait-
443 environment relationships suffer from inflated Type I error rate when CWMs include
444 (among-site) ITV in a similar way as when CWMs are calculated from fixed species-level
445 trait values. We also showed that the extent of this inflation decreases with increasing
446 amounts of ITV; for very low ITV magnitudes it approaches the inflation of trait –
447 environment relationships using fixed CWMs, while for high ITV magnitudes it is almost
448 non-existent (Fig. 3a). At the range of ITV magnitude observed in our real world dataset
449 (0.35-0.60), inflation remains strong. The newly introduced max test extended for ITV
450 proved to control Type I error rate for the full range of simulated ITV magnitude, and we
451 suggest to use it whenever exploring site-specific CWM -environment relationships. Indeed,
452 our simulation dataset suggests that levels of ITV need to be more than 3 times the amount of

453 interspecific trait variation before inflation becomes neglectable, so the test is likely to be
454 needed in most real data studies.

455 Our real world dataset is rather small concerning both the number of species (48) and
456 sites (25), and is also quite homogeneous in terms of environmental conditions (due to the
457 small spatial extent). Consequently, we would expect the magnitude of ITV in our study (0.3-
458 0.6, or 30-60%, respectively) to be less extensive than for more species-rich communities
459 across strong environmental gradients at large spatial scales. Surprisingly, other studies have
460 nonetheless found lower ITV magnitudes, both at local (15-33%, Jung et al. 2010) and global
461 scales for plant communities (32%, Siefert et al. 2015). It therefore seems unlikely that the
462 extent of ITV in a real datasets would be sufficiently high (>300%) to overcome type I error
463 inflation for site-specific CWM-environment relationships, without the use of a max test
464 correction, at least for plant communities. A detailed review of community-level studies
465 including ITV might be useful, however, to quantify the range of ITV magnitudes for
466 different taxa, environmental strengths and spatial scales. Also note that the comparison of
467 ITV magnitude with other studies is slightly hampered by the use of several alternative
468 measures for ITV magnitude (cf. Lepš et al. 2006, Albert et al. 2010, de Bello et al. 2011,
469 Siefert et al. 2015). We nonetheless expect ITV magnitude values to differ only slightly
470 among these different methods.

471 The use of trait values measured on the level of individual sites (“site-specific ITV”),
472 as in this study, is just one example of how ITV can be incorporated in CWM-based trait –
473 environment relationships. ITV covers any type of intraspecific trait variation, from variation
474 among leaves of a single tree to variation among individuals of a species occurring on
475 different continents. Specifically for CWM-based trait – environment relationships, the
476 amount of included ITV can gradually range from the inclusion of only ‘habitat- specific’ or
477 ‘region-specific’ ITV, where sites of one habitat or region are characterized by fixed species-

478 level trait values (e.g. Lepš et al. 2011, Helsen et al. 2018), to the inclusion of fine-scale
479 intra-site ITV (trait variation among individuals in a site) (e.g. Carlucci et al. 2015). The
480 severity of type I error inflation is expected to decrease along this gradient, since the more
481 detailed ITV information is included, the more likely ITV magnitude will be considerable.
482 Our study nonetheless suggests that Type I error corrections will remain necessary for any
483 study where the magnitude of ITV is lower than 3.

484 The actual level of Type I error inflation in real world datasets is also influenced by
485 several other parameters, next to the amount of ITV. As shown using a similar simulation
486 model as used in our study, inflation increases with decreasing beta diversity of the species
487 compositional data, increasing number of community samples used in the analysis and
488 increasing strength of the link between the environmental variable and the species
489 composition data (Zelený 2018). The strength of the **e-L** link in particular likely explains
490 why the inflation is high for site-specific CWM related to CA1 (which is intrinsically
491 strongly linked to the **L** matrix) and low when related to the real measured environmental
492 variable, windwardness (with has a much weaker link to matrix **L**). The newly introduced
493 ITV-extended max test nonetheless solved the inflated Type I error rate problem in both the
494 simulated and real data.

495 Surprisingly, the relationships between the intraspecific CWMs and environment
496 showed no Type I error inflation when tested with standard parametric tests. Even more, this
497 test appears to be conservative, with inflation rates being consistently lower than 1, in both
498 simulated data and real world data. We hypothesise that the lack of power is caused by the
499 way intraspecific CWMs are calculated: the matrix of site-specific trait values is converted
500 into the matrix of intraspecific trait values by centering the species' traits, resulting in
501 intraspecific trait values and CWM's which tend to have values close to zero, and thus very
502 low variance. In the case of our less noisy simulated dataset, this behaviour is quite

503 pronounced, resulting in low inflation index values (<0.4), while for the noisier real world
504 data this behaviour is less pronounced, with inflation index values only slightly below 1.
505 Detailed analyses should be performed in the future to uncover whether this is the real reason
506 for the apparent conservatism of the test.

507 Our study demonstrates the problem of Type I error inflation for site-specific
508 CWMs – environment relationships assessed specifically using linear regression. We assume,
509 however, that the same problem applies to other methods that can be used to assess trait-
510 environment relationships with the CWM approach, including correlation (parametric or non-
511 parametric), weighted regression (ter Braak et al. 2017) or ANOVA. Although not
512 specifically assessed in this study, we assume that our new ITV-extended max test can solve
513 this inflation in all of these methods, since they belong (or are closely related) to the same
514 statistical family of general linear models. As shown by ter Braak et al. (2017) for fixed
515 CWMs, the “original” max test is also applicable to this whole range of methods. It
516 nonetheless remains useful to formally evaluate the sensitivity of these different methods to
517 the Type I error rate inflation and their respective power.

518 In our analysis of trait-environment relationship on real cloud forest data, we
519 deliberately ignored the Type I error inflation problem associated with multiple testing,
520 which arises when conclusions are based on results of several (non-independent) tests carried
521 out on the same dataset. Note that this issue is independent of the Type I error rate inflation
522 explored in this study. When the CWM approach is used to identify multiple trait-
523 environment relationships, an additional correction of significance levels for this multiple
524 testing issue is necessary to avoid inflated family-wise Type I error rates (see Wright 1992).
525 We suggest to base this correction on the number of trait-environment pairs, not on the
526 overall number of tests performed; i.e. no matter whether the study focuses on only a single
527 CWM type (e.g. the site-specific one) or all three CWMs, each P-value should be adjusted by

528 the value calculated as the number of traits \times the number of environmental variables. The
529 correction for multiple testing will also require a higher number of permutations for each
530 individual test, as to allow the adjusted P -values to reach values lower than the selected
531 significance threshold (e.g. $\alpha = 0.05$).

532 **Practical considerations**

533 For researchers using the CWM approach extended for ITV, we suggest the following
534 workflow. From the three CWMs calculated within this extension, namely fixed, site-specific
535 and intraspecific CWM, only the first two are prone to Type I error inflation. For fixed
536 CWMs, we suggest using the original max (permutation) test, as introduced by Peres-Neto et
537 al. (2017), which is currently available in the *weimea* R package (Zelený, unpublished;
538 <https://github.com/zdealveindy/weimea>). For site-specific CWMs, the max test extended for
539 ITV as introduced in this study can be used, by applying the custom-made functions provided
540 in the R code accompanying this manuscript (https://github.com/zdealveindy/ITV_CWM).
541 For intraspecific CWMs, standard parametric tests do not suffer from Type I error rate
542 inflation and no correction is needed.

543 When using the results of previously published studies that applied the CWM
544 approach extended for ITV without controlling for Type I error inflation, be aware that some
545 of them may be overly optimistic. As previously shown for the CWM approach without
546 extension for ITV, Type I error inflation in fixed CWM-environment relationships correlate
547 positively with dataset size and strength of the link between species composition and
548 environment, and negatively with the overall species beta diversity (Zelený 2018). We show
549 that for assessing site-specific CWM-environment relationships using the CWM approach
550 extended for ITV, inflation is additionally negatively dependent on the magnitude of ITV.

551 **Acknowledgements**

552 Our thanks goes out to all members of the Vegetation Ecology Lab at the National Taiwan
553 University and several volunteers, who participated in the vegetation data collection
554 campaign of the Lalashan Forest Dynamics Plot, especially Ting Chen and Kun-Sung Wu.
555 This study was supported by a grant from the Taiwanese Ministry of Science and Technology
556 (MOST 109-2621-B-002-002-MY3).

557 **Supporting Information**

558 Appendix S1 with Figure S1 and S2

559 **Literature Cited**

560 Albert, C. H., W. Thuiller, N. G. Yoccoz, A. Soudant, F. Boucher, P. Saccone, and S. Lavorel.
561 2010. Intraspecific functional variability: extent, structure and source of variation.
562 *Journal of Ecology* 98:604–613.

563 Albert, C. H., F. de Bello, I. Boulangeat, G. Pellet, S. Lavorel, and W. Thuiller. 2012. On the
564 importance of intraspecific variability for the quantification of functional diversity.
565 *Oikos* 121:116–126.

566 Albert, C. H., F. Grassein, F. M. Schurr, G. Vieilledent, and C. Violle. 2011. When and how
567 should intraspecific variability be considered in trait-based plant ecology?
568 *Perspectives in Plant Ecology, Evolution and Systematics* 13:217–225.

569 Albert, C. H., W. Thuiller, N. G. Yoccoz, R. Douzet, S. Aubert, and S. Lavorel. 2010. A
570 multi-trait approach reveals the structure and the relative importance of intra- vs.
571 interspecific variability in plant traits. *Functional Ecology* 24:1192–1201.

- 572 Behm, J. E., and E. T. Kiers. 2014. A phenotypic plasticity framework for assessing
573 intraspecific variation in arbuscular mycorrhizal fungal traits. *Journal of Ecology*
574 102:315–327.
- 575 Borgy, B., et al. 2017. Sensitivity of community-level trait–environment relationships to data
576 representativeness: A test for functional biogeography. *Global Ecology and*
577 *Biogeography* 26:729–739.
- 578 Brown, A. M., D. I. Warton, N. R. Andrew, M. Binns, G. Cassis, and H. Gibb. 2014. The
579 fourth-corner solution –using predictive models to understand how species traits
580 interact with the environment. *Methods in Ecology and Evolution* 5:344–352.
- 581 Candeias, M., and J. Fraterrigo. 2020. Trait coordination and environmental filters shape
582 functional trait distributions of forest understory herbs. *Ecology and Evolution*
583 10:14098–14112.
- 584 Carlucci, M. B., V. J. Debastiani, V. D. Pillar, and L. D. S. Duarte. 2015. Between- and
585 within-species trait variability and the assembly of sapling communities in forest
586 patches. *Journal of Vegetation Science* 26:21–31.
- 587 Condit, R. 1998. *Tropical forest census plots: methods and results from Barro Colorado*
588 *Island, Panama and a comparison with other plots*. Springer, Berlin, Germany.
- 589 Cormont, A., C. C. Vos, C. A. M. van Turnhout, R. P. B. Foppen, and C. J. F. ter Braak. 2011.
590 Using life-history traits to explain bird population responses to changing weather
591 variability. *Climate Research* 49:59–71.
- 592 Curtis, J. T. 1959. *The vegetation of Wisconsin: an ordination of plant communities*.
593 University of Wisconsin Press, Madison, WI, US.
- 594 Dawson, S. K., and M. Jönsson. 2020. Just how big is intraspecific trait variation in
595 basidiomycete wood fungal fruit bodies? *Fungal Ecology* 46: 100865.

- 596 Díaz, S., S. Lavorel, F. de Bello, F. Quétier, K. Grigulis, and T. M. Robson. 2007.
597 Incorporating plant functional diversity effects in ecosystem service assessments.
598 Proceedings of the National Academy of Sciences of the United States of America
599 104:20684–20689.
- 600 Dray, S., and P. Legendre. 2008. Testing the species traits-environment relationships: The
601 fourth-corner problem revisited. *Ecology* 89:3400–3412.
- 602 Fajardo, A., and A. Siefert. 2018. Intraspecific trait variation and the leaf economics
603 spectrum across resource gradients and levels of organization. *Ecology* 99:1024–1030.
- 604 Fridley, J. D., D. B. Vandermast, D. M. Kuppinger, M. Manthey, and R. K. Peet. 2007. Co-
605 occurrence based assessment of habitat generalists and specialists: A new approach
606 for the measurement of niche width. *Journal of Ecology* 95:707–722.
- 607 Garnier, E., et al. 2004. Plant functional markers capture ecosystem properties during
608 secondary succession. *Ecology* 85:2630–2637.
- 609 Gaudard, C. A., M. P. Robertson, and T. R. Bishop. 2019. Low levels of intraspecific trait
610 variation in a keystone invertebrate group. *Oecologia* 190:725–735.
- 611 Helsen, K., et al. 2018. Impact of an invasive alien plant on litter decomposition along a
612 latitudinal gradient. *Ecosphere* 9:e02097.
- 613 Jamil, T., W. A. Ozinga, M. Kleyer, and C. J. F. ter Braak. 2013. Selecting traits that explain
614 species-environment relationships: A generalized linear mixed model approach.
615 *Journal of Vegetation Science* 24:988–1000.
- 616 Jung, V., C. H. Albert, C. Violle, G. Kunstler, G. Loucougaray, and T. Spiegelberger. 2010.
617 Intraspecific trait variability mediates the response of subalpine grassland
618 communities to extreme drought events. *Journal of Ecology* 102:45–53.
- 619 Keddy, P. A. 1992. Assembly and response rules: two goals for predictive community
620 ecology. *Journal of Vegetation Science* 3:157–164.

- 621 Lavorel, S., and E. Garnier. 2002. Predicting changes in community composition and
622 ecosystem functioning from plant traits: Revisiting the Holy Grail. *Functional*
623 *Ecology* 16:545–556.
- 624 Legendre, P., R. Galzin, and M. L. Harmelin-Vivien. 1997. Relating behavior to habitat:
625 Solutions to the fourth-corner problem. *Ecology* 78:547–562.
- 626 Lennon, J. J. 2000. Red-shifts and red herrings in geographical ecology. *Ecography* 23:101–
627 113.
- 628 Lepš, J., F. de Bello, P. Šmilauer, and J. Doležal. 2011. Community trait response to
629 environment: Disentangling species turnover vs intraspecific trait variability effects.
630 *Ecography* 34:856–863.
- 631 Li, C.-F., et al. 2013. Classification of Taiwan forest vegetation. *Applied Vegetation Science*
632 16:698–719.
- 633 McGill, B. J., B. J. Enquist, E. Weiher, and M. Westoby. 2006. Rebuilding community
634 ecology from functional traits. *Trends in Ecology and Evolution* 21:178–185.
- 635 Messier, J., B. J. McGill, and M. J. Lechowicz. 2010. How do traits vary across ecological
636 scales? A case for trait-based ecology. *Ecology Letters* 13:838–848.
- 637 Miller, J. E. D., E. I. Damschen, and A. R. Ives. 2019. Functional traits and community
638 composition: A comparison among community-weighted means, weighted
639 correlations, and multilevel models. *Methods in Ecology and Evolution* 10:415–425.
- 640 Minchin, P. 1987. Simulation of multidimensional community patterns: towards a
641 comprehensive model. *Vegetatio* 71:145–156.
- 642 Peres-Neto, P. R., S. Dray, and C. J. F. ter Braak. 2017. Linking trait variation to the
643 environment: Critical issues with community-weighted mean correlation resolved by
644 the fourth-corner approach. *Ecography* 40:806–816.

- 645 Pérez-Harguindeguy, et al. 2013. New handbook for standardised measurement of plant
646 functional traits worldwide. *Australian Journal of Botany* 61:167–234.
- 647 R Core Team. 2021. R: A language and environment for statistical computing. R Foundation
648 for Statistical Computing, Vienna, Austria. URL <https://www.R-project.org/>.
- 649 Sandel, B., and R. Low. 2019. Intraspecific trait variation, functional turnover and trait
650 differences among native and exotic grasses along a precipitation gradient. *Journal of*
651 *Vegetation Science* 30:633–643.
- 652 Siefert, A., et al. 2015. A global meta-analysis of the relative extent of intraspecific trait
653 variation in plant communities. *Ecology Letters* 18:1406–1419.
- 654 Taudiere, A., and C. Violle. 2015. cati: an R package using functional traits to detect and
655 quantify multi-level community assembly processes. *Ecography* 39:699–708.
- 656 ter Braak, C. J. F., A. Cormont, and S. Dray. 2012. Improved testing of species traits-
657 environment relationships in the fourth-corner problem. *Ecology* 93:1525–1526.
- 658 ter Braak, C. J. F., P. Peres-Neto, and S. Dray. 2018. Simple parametric tests for trait-
659 environment association. *Journal of Vegetation Science* 29:801–811.
- 660 Valencia, R., et al. 2004. Tree species distributions and local habitat variation in the Amazon:
661 large forest plot in eastern Ecuador. *Journal of Ecology* 92:214–229.
- 662 Violle, C., B. J. Enquist, B. J. McGill, L. Jiang, C. H. Albert, C. Hulshof, V. Jung, and J.
663 Messier. 2012. The return of the variance: intraspecific variability in community
664 ecology. *Trends in Ecology and Evolution* 27:244–252.
- 665 Violle, C., M. M.-L. Navas, D. Vile, E. Kazakou, C. Fortunel, I. Hummel, and E. Garnier.
666 2007. Let the concept of trait be functional! *Oikos* 116:882–893.
- 667 Warton, D. I., B. Shipley, and T. Hastie. 2015. CATS regression -a model-based approach to
668 studying trait-based community assembly. *Methods in Ecology and Evolution* 6:389–
669 398.

- 670 Westerband, A. C., J. L. Funk, and K. E. Barton. 2021. Intraspecific trait variation in plants: a
671 renewed focus on its role in ecological processes. *Annals of Botany* 127:397–410.
- 672 Wright, S. P. 1992. Adjusted *P*-values for simultaneous inference. *Biometrics* 48:1005–1013.
- 673 Zelený, D. 2018. Which results of the standard test for community weighted mean approach
674 are too optimistic? *Journal of Vegetation Science* 29: 953–966.
- 675 Zobel, M., E. van der Maarel, and C. Dupré. 1998. Species pool: the concept, its
676 determination and significance for community restoration. *Applied Vegetation*
677 *Science* 1:55–66.
- 678
- 679

680 **Tables**

681 Table 1. Leaf traits of woody species in the cloud forest: regression of site-specific (SS), fixed (F) and intraspecific (ITV) CWM on
 682 environmental variables, tested by parametric F -test (P_{par}) and max permutation test (P_{max} ; ITV-extended max test was used for site-specific
 683 CWM, and “original” max test for fixed CWM). Significant results ($P < 0.05$) are in bold.

684

Environmental variable	CWM type	LA				Lth				SLA				LDMC			
		r^2	F	P_{par}	P_{max}	r^2	F	P_{par}	P_{max}	r^2	F	P_{par}	P_{max}	r^2	F	P_{par}	P_{max}
elevation	SS	0.101	2.58	0.122	0.179	0.025	0.60	0.448	0.518	0.001	0.01	0.911	0.923	0.018	0.42	0.523	0.628
	F	0.166	4.58	0.043	0.095	0.035	0.85	0.367	0.497	0.002	0.05	0.822	0.881	0.003	0.07	0.799	0.860
	ITV	0.006	0.15	0.704		0.011	0.25	0.624		0.000	0.01	0.940		0.061	1.48	0.236	
convexity	SS	0.031	0.73	0.403	0.442	0.073	1.82	0.190	0.218	0.066	1.63	0.215	0.252	0.008	0.18	0.678	0.691
	SS	0.030	0.70	0.411	0.486	0.024	0.56	0.461	0.549	0.164	4.50	0.045	0.091	0.120	3.14	0.089	0.154
	ITV	0.004	0.08	0.778		0.089	2.25	0.147		0.003	0.06	0.810		0.033	0.79	0.384	
windwardness	SS	0.120	3.13	0.090	0.104	0.285	9.18	0.006	0.007	0.370	13.50	0.001	0.003	0.001	0.02	0.890	0.909
	F	0.035	0.84	0.369	0.488	0.054	1.31	0.265	0.364	0.065	1.60	0.219	0.311	0.018	0.43	0.520	0.609
	ITV	0.172	4.79	0.039		0.412	16.13	0.001		0.431	17.41	0.000		0.006	0.14	0.710	

685

686

687 **Figures**

688 **Figure 1.** The schema of (a) the row-based and (b) the column-based permutation test for
689 fixed trait values CWM. Resulting *P*-values from both tests are combined into the max test.
690 Grey cells represent values of non-zero species abundances (in species composition matrix **L**
691 and **P**) or values of traits and environmental variables that are not missing.

692

693 **Figure 2.** The schema of ITV-extended max test. (a) The row-based permutation test for site-
694 specific trait values. (b) Combined column-based permutation test, with separate permutation
695 of fixed trait values and intraspecific trait values. Max test combines *P*-values from both tests
696 by selecting the higher one. Grey cells represent values of non-zero species abundances (in
697 species composition matrix **L** and **P**) or values of traits and environmental variables which
698 are not missing.

699

700 **Figure 3.** The effect of the magnitude of intraspecific trait variation (relative ITV index) on
701 inflation index (mean + standard deviation) of the linear regression between (a, c) site-
702 specific CWM or (b) intraspecific CWM and the ‘environmental variable’ of the simulated
703 data, tested by (a, b) standard parametric test and (c) “max” permutation test. Black square =
704 fixed CWM (cf. site-specific CWM with no ITV). Relative ITV index equal to infinity (∞)
705 represents situation when site-specific trait matrix with trait values randomly sampled from
706 normal distribution was used. No inflation occurs if the inflation index is equal or lower to 1
707 (indicated by dashed horizontal line).

708

709 **Figure 4.** The effect of the magnitude of intraspecific trait variation (relative ITV index) on
710 inflation index (mean + standard deviation) of the linear regression between (a, c) site-

711 specific CWM or (b) intraspecific CWM and windwardness (gray italics) and CA1 (black) of
712 the cloud forest data, tested by (a,b) standard parametric test and (c) “max” permutation test.
713 No inflation occurs if the inflation index is equal or lower to 1 (indicated by dashed
714 horizontal line). LA = leaf area, SLA = specific leaf area, LDMC = leaf dry matter content,
715 Lth = leaf thickness.

716

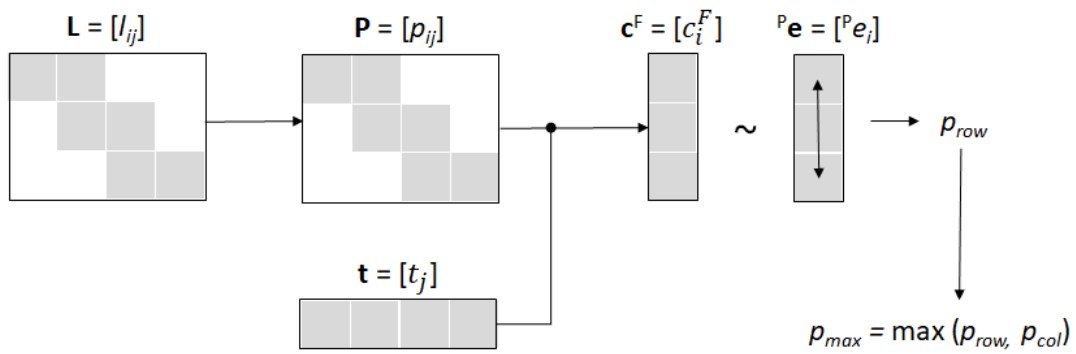
717 **Figure 5.** Regression between windwardness and the site-specific, fixed and intraspecific
718 CWM of (a) leaf area, (b) leaf thickness, and (c) specific leaf area. All CWMs were z-
719 transformed. Regressions significant at $P < 0.05$ (max test in the case of site-specific and
720 fixed CWM, parametric test in the case of intraspecific CWM) were visualized by a solid
721 regression line, non- significant regressions by a dashed line.

722

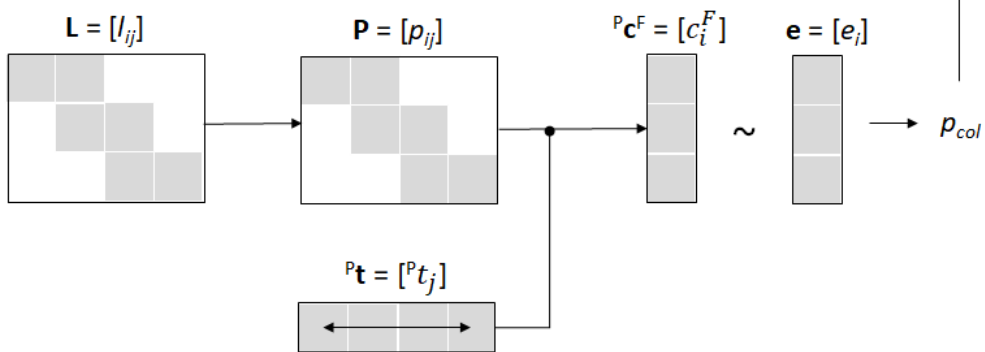
723 Figure 1

724

(a) Row-based permutation test



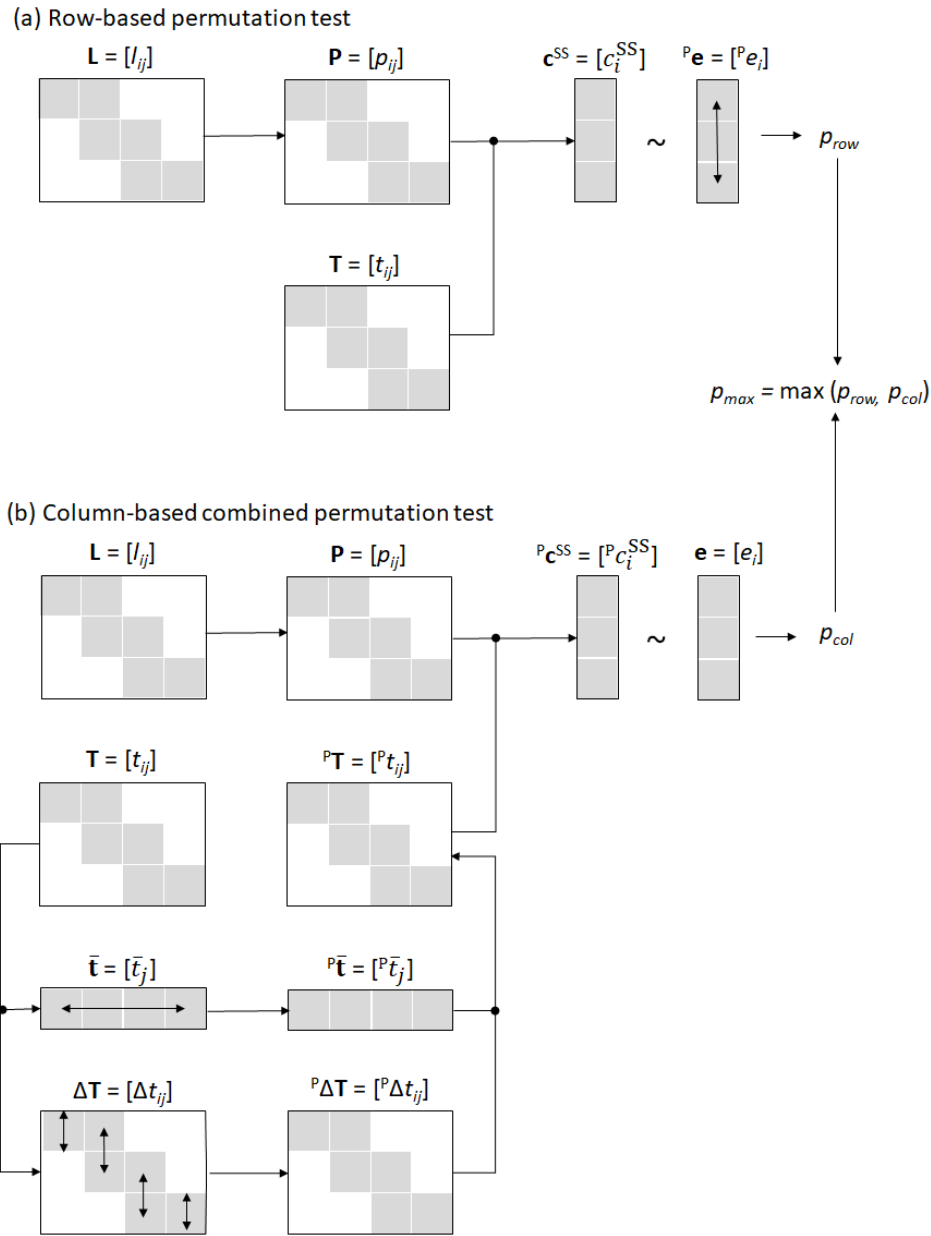
(b) Column-based permutation test



725

726

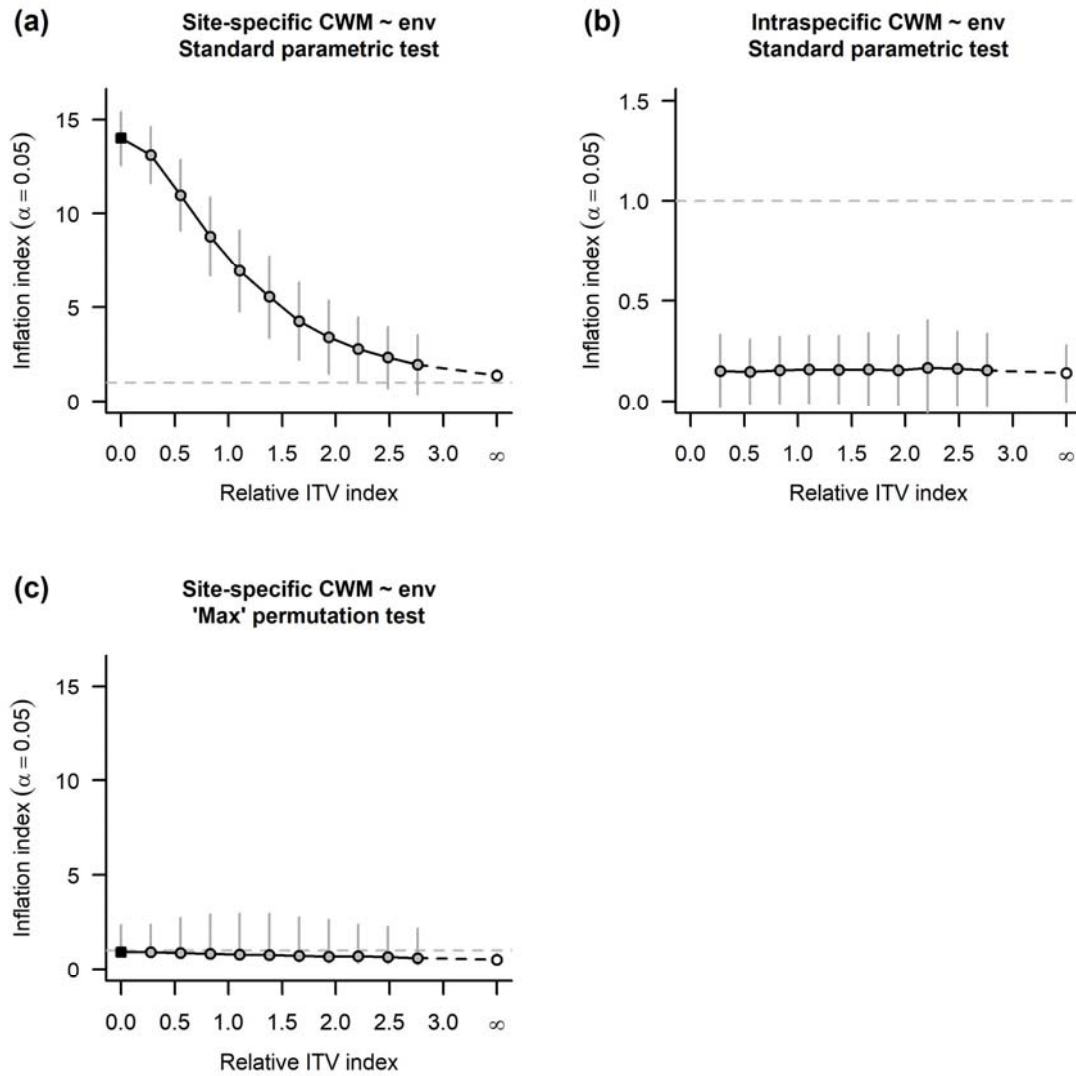
727 Figure 2



728

729

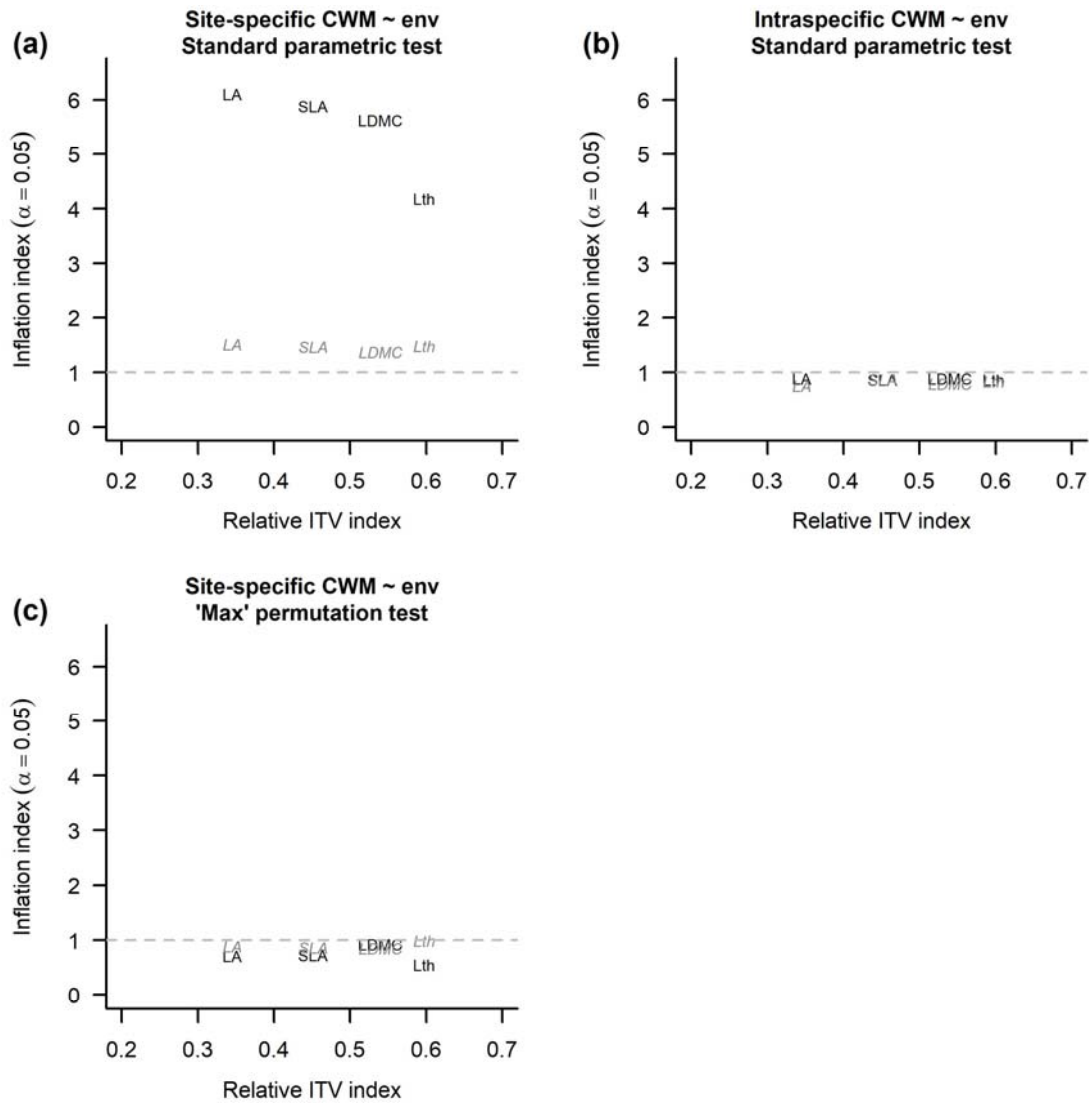
730 Figure 3



731

732

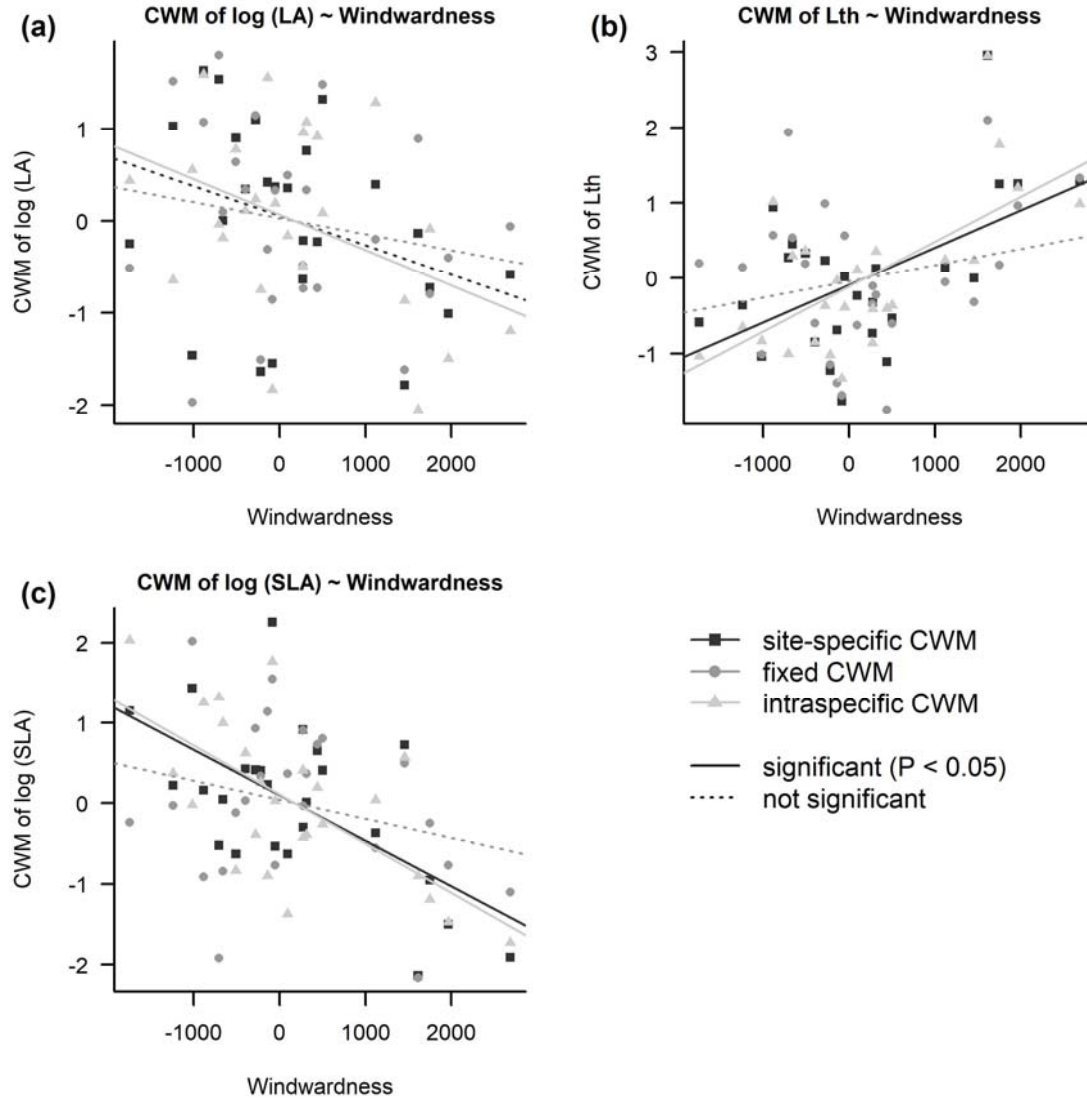
733 Figure 4



734

735

736 Figure 5



737